Materials Research. 2019; 22(4): e20180917
DOI: http://dx.doi.org/10.1590/1980-5373-MR-2018-0917

Biomimetic Coating of Mechanochemically Synthesized Zirconium Titanate

David Rentería-Zamarrón[a]*, Jose Alonso Díaz-Guillén[a], Dora Alicia Cortés-Hernández[b], Sagrario Martinez-Montemayor[c], Claudia Magdalena Lopez-Badillo[d], Antonio Fernandez-Fuentes[b]

[a]División de Estudios de Posgrado e Investigación, Tecnológico Nacional de México, Instituto Tecnológico de Saltillo, Saltillo, Coahuila, México
[b]Departamento de Ingeniería Cerámica, Centro de Investigación y de Estudios Avanzados del IPN (CINVESTAV), Saltillo, Coahuila, México
[c]Departamento de Materiales Avanzados, Centro de Investigación en Química Aplicada (CIQA), Saltillo, Coahuila, México
[d]Facultad de Ciencias Químicas, Universidad Autónoma de Coahuila - UAdeC, Saltillo, Coahuila, México

Received: December 20, 2018; Revised: April 08, 2019; Accepted: May 19, 2019

A biomimetic method was used to promote bioactivity of $ZrTiO_4$. Zirconium titanate was obtained by using a combination of techniques such as mechanical milling and heat treatment of zirconia and titania powders. The effect of milling time on the evolution of the $ZrTiO_4$ phase formation was studied. Powders were uniaxially pressed followed by heat treatment for 6 h at different temperatures within the range between 700 and 1500 ºC. Single phase $ZrTiO_4$ was obtained after ball-milling for 30 h followed heat treating in air at 1500 ºC for 6 h. For the biomimetic coatings were obtained by immersion of the samples in a simulated body fluid (SBF) for 7, 14 and 21 days on a bed of wollastonite powder, and were characterized by SEM, EDS, XRD, FT-IR and TEM. For comparison purposes, experiments were also performed without using the bioactive powder bed. A bone-like apatite layer was formed on zirconium titanate after 21 days of immersion in SBF using a bed of wollastonite powder.

Keywords: *zirconium titanate, biomaterials, biomimetic method, HA coating, mechanical milling.*

1. Introduction

The biomaterials science has gained great importance because the human being wanted to improve their quality of life. The sophistication of implants and prostheses in recent years has led to the development of new materials with the necessary requirements to biomedical applications. And to gather the required properties in a single material, which have become the greatest challenge of our times [1]. And one of these possible materials can be composed of ZrO_2 and TiO_2, such as zirconium titanate, which we will now talk about its characteristics both electric, and biocompatibility. Zirconium titanate is a material that has the potential for such application, due to its high performance, good stability at high temperature and high resistance to heat and corrosive environment; it is widely used in electronic components, that is, for telecommunication purposes such as resonators, capacitors, etc. [2]. Different methods have been employed to prepare zirconium titanate ceramic materials such as solid state reaction method, high energy ball milling, DC magnetron sputtering, co-precipitation, sol-gel and mechanochemical processing [3]. Mechanochemical processing has become very popular since it is a simple method to employ, in which there is no need to use solvents and with which sufficient volume of the material to be treated can be obtained in an economically viable manner [4].

As mentioned previously, zirconium titanate is a material that has great qualities such as, high performance, good stability at high temperature and high resistance to heat and corrosive environment; and the compound may crystallize in the orthorhombic system, which is related to its electrical properties. The zirconium and titanium ions are distributed randomly occupying octahedral sites [5]. The traditional scope of zirconium titanate materials is that of electroceramics, as dielectric resonators due to their high dielectric constant ($\kappa \approx$ 35-46), high quality factor ($Q \approx$ 2000-8000) measured between 1 and 10 GHz and their small variation of the resonance frequency with temperature ($\tau f \approx 0$ ppm $ºC^{-1}$) [6-15]. These properties make the zirconium titanate materials useful in the field of telecommunications as tuners, filters and voltage oscillators tuneable by voltage [6,11]. In addition, the dielectric properties of zirconium titanate have been determined in thin films prepared by laser ablation [11]. On the other hand, zirconium titanate materials are used in catalytic applications. Zirconium titanate has catalytic activity in some reactions, such as the non-oxidative dehydrogenation of ethylbenzene, which is important in the production of styrene. Likewise, it has been used in a large number of catalytic reactions as catalyst support[12-15]. In addition, zirconium titanate has photocatalytic activity. Applications of zirconium titanate as a pigment [16] and as a hydrocarbon (methane, propane, toluene and hexane) [13,17] and humidity sensor have also been described [18,19].

*e-mail: drenteria@itsaltillo.edu.mx

On the other hand, zirconia has been used in combination with other oxides such as SiO_2 and Al_2O_3; studies on biological behaviour have shown that zirconia and silica create favourable non-toxic layers with good biocompatibility [20]. In addition, ZrO_2 exhibits high mechanical strength, high fracture resistance and corrosion, making it a suitable material for implants [21]. Zirconium dioxide (ZrO_2) is a bioinert ceramic material generally known for its excellent mechanical strength and hardness. Materials based on both ZrO_2 and Al_2O_3 are considered bioinert under physiological conditions and, therefore, in surface modification treatments [21]. Due to the excellent biocompatibility of titanium dioxide (TiO_2), recent studies have shown the manufacture of a highly porous ceramic material (scaffolding) from TiO_2 foams for bone growth and the ability to promote adhesion and proliferation of osteoblasts and mesenchymal cells (hMSC) on the entire surface of the scaffold in in vitro testing [20,21]. On the other hand, crystalline TiO_2 has shown to have bioactive properties since its surface can support chemical bonds with bone, through the formation of an apatite layer similar to that of bone; however it lacks mechanical strength and hardness of ZrO_2. Therefore, combining the favourable osteogenic properties of TiO_2 with the excellent mechanical properties of ZrO_2 may allow the manufacture of osteoconductive materials with sufficient mechanical strength to withstand the stress to which they will be subjected, while maintaining biocompatibility [20,21].

Biomimetic processes have been widely studied for growing a bonelike apatite layer on different substrates by immersion in simulated body fluids. In the case of the wollastonite, calcium ions released into the solution increase the ionic activity product of the apatite in the fluid and the Si-OH groups formed on the surface provide sites for apatite nucleation [22]. After the apatite nuclei are formed, they grow spontaneously since the solution is already saturated with respect to apatite. In this case, calcium and silicate ions dissolved from the bioactive material induce apatite nucleation on the materials placed nearby [20,22].

The aim of this study is to obtain the $ZrTiO_4$ ceramic material by mechanical milling followed by heat treatment, with the possibility of being used as a biomaterial. And so to face the problem of corrosion in physiological fluids that have certain metals and alloys, when used as implants in the body. The effects of milling time and heat treatment temperature on the evolution of the $ZrTiO_4$ formation are presented. In addition, selected samples were biomimetically treated on views to the potential use of this materials in biomedical applications, such as orthopaedic and dental implants.

2. Experimental

2.1 Zirconium titanate preparation

Single phase $ZrTiO_4$ materials were prepared by mechanical milling. This powder processing method has already been successfully used to prepare zirconate and titanate materials at room temperature [4,23]. Stoichiometric mixtures of high-purity (≥ 99%, Sigma Aldrich) TiO_2 and ZrO_2 reagent grade chemicals were placed into zirconia containers along with 20 mm diameter zirconia balls as grinding media (balls to powder mass ratio = 10:1). Dry mechanical milling was carried out in air in a planetary ball mill using a rotating disc speed of 400 rpm for different milling times (1, 3, 6, 20 and 30 h). Phase evolution on milling was periodically analyzed by X-Ray Diffraction (XRD) in a Philips X'pert diffractometer (0.01º/s) using Ni-filtered CuKα radiation (λ=1.5418 Å) and reactions were considered complete when no traces of the starting reagents were evident by this technique. Pills (10 mm diameter and ~1 mm thickness) were obtained by uniaxial pressing (38 MPa for 20 sec) of the fine powders prepared by mechanical milling. To increase their mechanical strength and obtain dense samples, pills were heat treated at different temperatures 700, 1000 and 1500 ºC for 6 h (heating and cooling rates 2 ºC/min).

2.2 Biomimetic method

A Simulated Body Fluid (SBF) with ionic concentration nearly equal to that of human blood plasma (SBF) was used. The solution was prepared according to Kokubo´s recipe [24], dissolving reagent grade sodium chloride (NaCl), sodium hydrogen carbonate ($NaHCO_3$), potassium chloride (KCl), dipotassium hydrogen phosphate ($K_2HPO_4 \cdot 3H_2O$), magnesium chloride hexahydrate ($MgCl_2 \cdot 6H_2O$), calcium chloride dihydrate ($CaCl_2 \cdot 2H_2O$) and sodium sulfate (Na_2SO_4) in deionized water and buffered with tri(hydroxymethyl)-aminomethane and 1N HCl at 36.5 ºC. The substrates were washed with acetone and deionized water, and then immersed in 150 mL of SBF at 36.5 ºC in an incubator, and under static conditions. The biomimetic coatings were obtained by the immersion of samples in SBF for 7, 14 and 21 days with or without the presence of a bed of wollastonite powder, as a calcium ions supplier, these ions are released into the SBF increasing the ionic activity, which generates the formation of apatite on the surface of the materials that contain it. The pills of the material were placed on a wollastonite bed in a container, one face of the pill was on the wollastonite bed, and the other face was exposed to the contact with the fluid. After immersion periods, substrates were removed from the bottles, gently washed with deionized water and dried at room temperature [22, 24].

The surface of the biomimetically treated substrates was analyzed by X-Ray Diffraction (XRD) (Philips, X'Pert), then substrates were Au-Pd coated and analyzed by Scanning Electron Microscopy (SEM) (Philips, XL-30 ESEM) and Energy Dispersive Spectroscopy (EDS) (Philips, XL-30 ESEM). Microstructural studies were also performed using High-Resolution Transmission Electron Microscopy (HRTEM) (FEI TITAN HRTEM), while Infrared spectroscopy (IR, NICOLET 500) was employed to assess the growth of the phosphate groups $(PO_4)^{3-}$, which are characteristics groups of apatite.

3. Results and Discussion

The evolution of the $ZrTiO_4$ phase as a function of milling time can be observed in Figure 1, which shows the XRD patterns of samples after different milling times (1, 3, 6, 20 and 30 h). For comparison purposes, the starting mixture is also included. The XRD pattern reported in the International Centre for Diffraction Data, ICDD (PDF 49-1642) for the fluorite cubic structure of ZrO_2, was used as reference. The characteristic reflections of the anatase-TiO_2 (PDF 00-078-2486) are also shown.

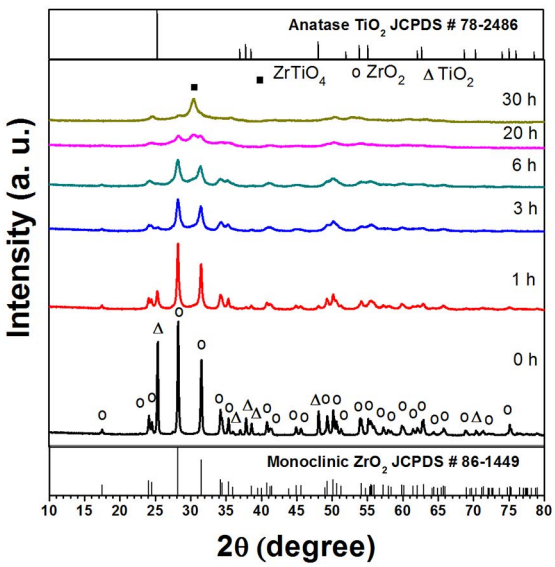

Figure 1. XRD patterns of samples after different milling times.

An important decreasing in intensity and broadening of the characteristic reflections of starting oxides are observed after the first 3 h of milling as a consequence of a considerable decrease in particle size and the introduction of a large number of structural defects due to the impact of balls to the powders. After 6 h of milling, XRD patterns show no appreciable changes. After 30 h, the powder mixture shows a pattern where the main reflection of the $ZrTiO_4$ (PDF 00-01-080- 6058) is evident. Reflections of remnant TiO_2 and ZrO_2 are also present. The width and low intensity of these reflections is related with the high structural disorder in these materials generated by mechanical activation. This pattern also reveals a slight increase of the reflections intensity with respect to the sample milled for 20 hours, which is practically amorphous. Either the crystallites growth of the formed phase or the increase in their number with milling time may be the cause for this effect. The presence of remnant reflections of starting reagents after 30 hours of milling made necessary a thermal treatment to complete the reaction of this mechanically activated composition.

Figure 2 shows the effect of heat treatment temperature on the structural characteristics of the Ti-Zr materials. Figure 2a shows XRD patterns of ball-milled samples for 30 h followed by heat treatment at different temperatures (700-1000 ºC) for 6 h. As observed, as the heat treatment temperature is increased, an increase in the reflections intensity and a decrease in their width are observed, leading to a material with high crystallinity and crystallite size. It is also clear that patterns of fired samples correspond to the $ZrTiO_4$ phase.

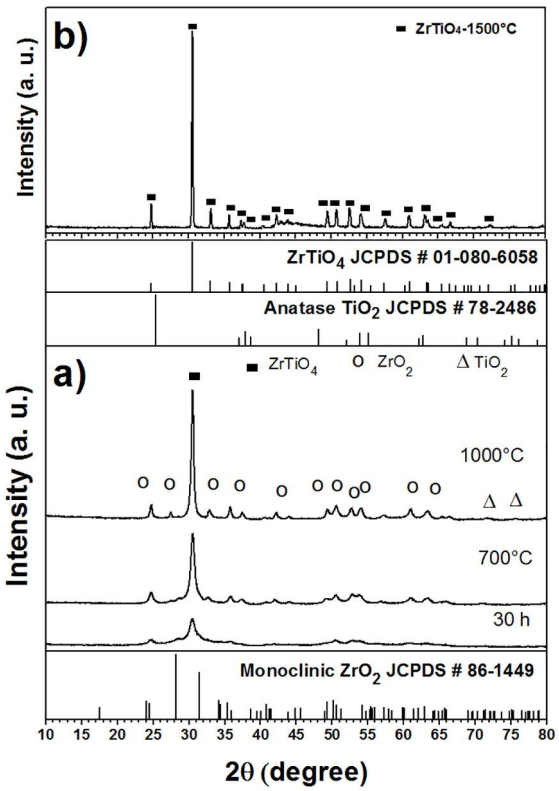

Figure 2. XRD patterns of balled-milled samples for 30 h treated at different temperatures for 6 h, (a) 700-1000 ºC, and (b) 1500 ºC.

Figure 2b shows the XRD pattern of the ball-milled sample for 30 h after heat treatment at 1500 ºC for 6 h. A single and highly crystalline phase, identified as $ZrTiO_4$ (PDF 00-01-080- 6058), was observed.

Figure 3 shows SEM images of the studied composition at different magnifications after 30 h of milling and sintered at 1500 °C for 6 h. It is a well densified microstructure with dispersed grain sizes. The corresponding EDS spectrum confirms the presence of Pd, because the sample was coated with this to be analyzed.

Figure 4 shows SEM images of sintered (1500 °C) $ZrTiO_4$ after 7, 14 and 21 days of immersion in SBF without using a wollastonite powder bed. As observed, no microstructural changes are observed, that is, there is no indication of the formation of a Ca, P-rich layer on the surface; this is probably due to the fact that the material is constituted by ZrO_2, which is already known as a bioinert material [22,24]. The EDS spectra confirm the presence of mainly Zr and Ti. During the immersion of bioinert samples in SBF, with no wollastonite powder bed, the nuclei formed are not able to grow since an excess of Ca and P ions is necessary. Thus, the nuclei formed tend to dissolve again [22,24]. Zirconium dioxide (ZrO_2) is a biocompatible ceramic material generally known for its excellent mechanical strength and toughness. However, this material is considered bioinert under physiological conditions, and therefore surface modification treatments, such as calcium phosphate coatings, are necessary to produce a bioactive material surface which may allow direct contact between the material surface and bone tissue without fibrous encapsulation [20,22,24,25]. However, some authors suggest that ZrO_2 is bioactive, because the ZrO_2 with tetragonal structure has presented apatite formation on its surface, it is also mentioned that in the presence of nanometer-sized particles of ZrO_2 it is also possible to make bioactive material; it is believed to be one of the reasons why the ZrO_2 is bioactive in comparison with ZrO_2 ceramics, which is considered bioinert [26].

According to the results presented above, the sample selected for biomimetic treatment was that ball-milled for 30 h and heat treated at 1500 ºC. Figure 5 shows SEM images of $ZrTiO_4$ after 7, 14 and 21 days of immersion in SBF in the presence of a wollastonite powder bed. The EDS spectrum of the sample corresponding to 7 days of immersion (Fig. 5a) demonstrates that the compound formed on the surface contains calcium and silicon due to the presence of the wollastonite powder bed used as a supplier of calcium ions. This wollastonite powder may play an important role in the nucleation and growth of bioactive crystals in the next stages of immersion.

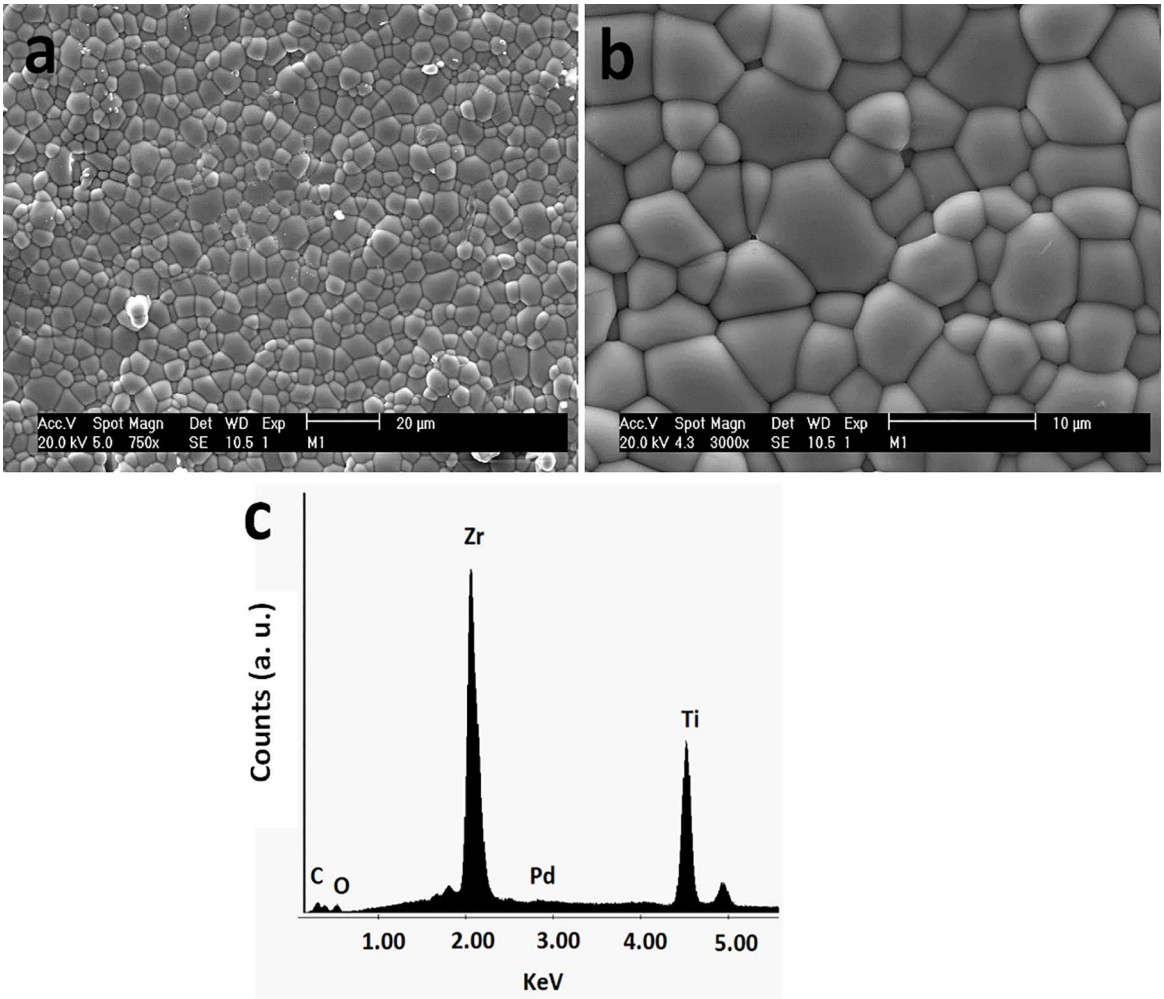

Figure 3. SEM images of sintered (1500 °C) $ZrTiO_4$ samples. Microstructures (a and b) and EDS spectrum (c).

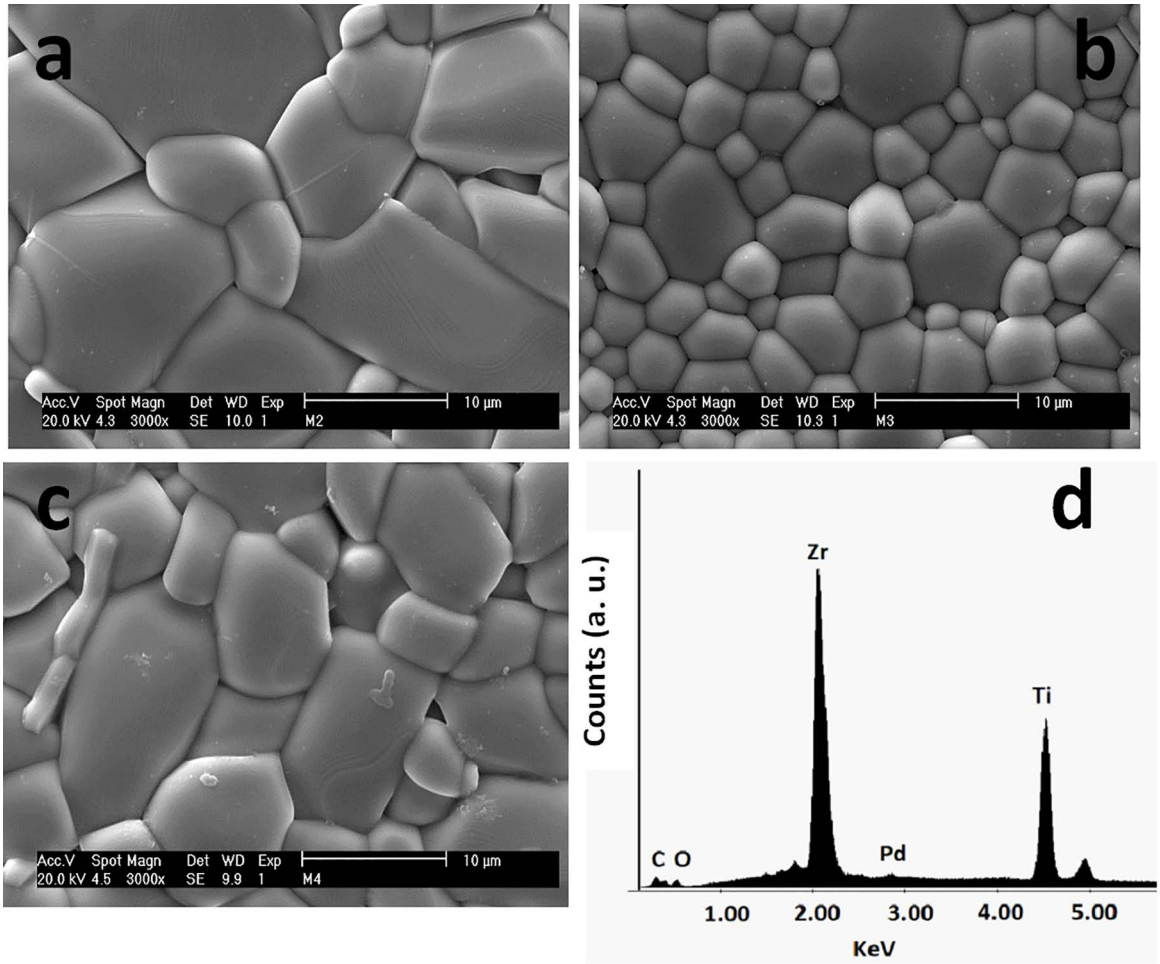

Figure 4. SEM images and EDS spectrum of sintered (1500 °C) $ZrTiO_4$ after 7 (a), 14 (b) and 21 days (c) of immersion in SBF without using a wollastonite powder bed.

After 14 days of immersion in SBF (Fig. 5b), a new compound, with a microstructure consisting of agglomerates of a smaller size than that of the $ZrTiO_4$ grains, has been formed. According to the corresponding EDS spectrum, even though the Zr peak overlaps with that of P, the elements detected, apart from those of the substrate, are Ca, P and Si.

After 21 days of immersion in SBF, a homogeneous Ca, P-rich layer has been formed on the surface, this according to the corresponding EDS spectrum (Fig. 5c). Silicon is also detected in a lower quantity than that corresponding to the sample immersed for 14 days (Fig. 5b). This may indicate that the wollastonite particles that were observed on the sample after 7 and 14 days of immersion have been dissolved into the SBF and an ionic exchange between H^+, from the SBF, and Ca^{2+}, from the wollastonite powder, takes place. This eventually increases pH and the ionic activity product of Ca and P ions in solution, leading to the nucleation and growth of the Ca, P-rich compound.

On the other hand, if a wollastonite bed is not used during the immersion of samples in SBF for 21 days, no changes were observed on the material surface [24].

Figure 6 shows the FT-IR spectra of the untreated sample (before immersion in SBF), the sample after 21 d of immersion in SBF and the biomimetically-treated sample after 21 d of immersion in SBF on a bed of wollastonite powder. Regarding to the untreated $ZrTiO_4$, the absorption band at 466 cm^{-1} corresponds to the vibration of the Zr-O bond and the absorption bands at 650 and 520 cm^{-1} correspond to Ti-O and Zr-O-Ti groups, respectively [25]. The spectrum of the sample immersed in SBF with no wollastonite powder bed is similar to that of the untreated $ZrTiO_4$ sample. In the FT-IR spectrum of the biomimetically treated sample, the absorption band at 574 cm^{-1} correspond to $(PO_4)^{3-}$ groups, several authors report the most intense signal of hydroxyapatite, the antisymmetric vibration of calcium phosphates υ3as$(PO4)^{3-}$ at 1040 and 1091 cm^{-1}. [26-28] and the stretching bands at 3645 and 2930 cm^{-1} correspond to O-H.

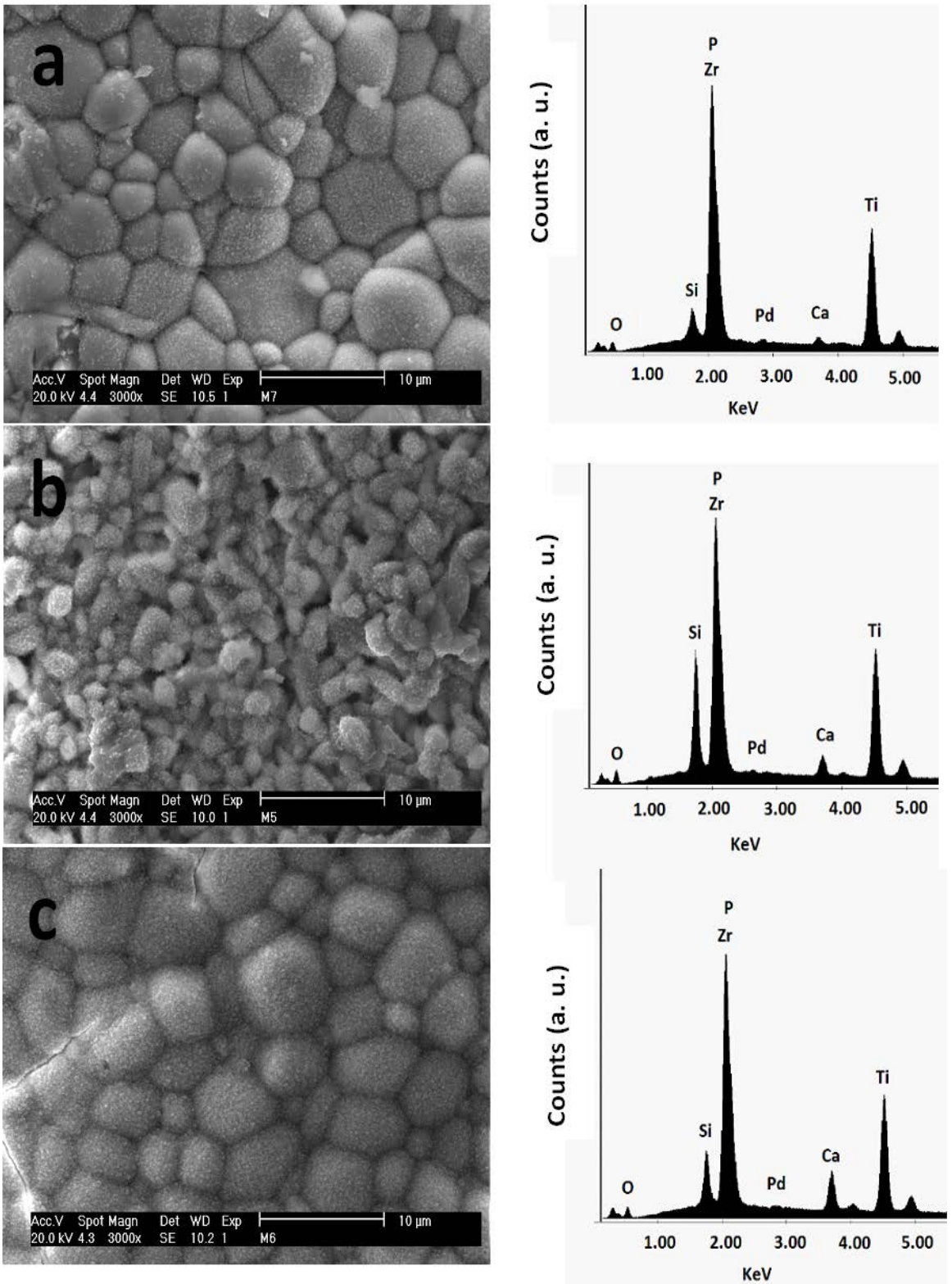

Figure 5. SEM images and EDS spectra of sintered (1500 °C) $ZrTiO_4$ after 7 days (a), 14 days (b) and 21 days (c), of immersion in SBF on a wollastonite powder bed.

These results are in agreement with those obtained by SEM and EDS and the presence of $(PO_4)^{3-}$ and O-H groups may indicate the formation of a bioactive compound on $ZrTiO_4$ after 21 days of immersion in SBF on a bed of wollastonite powder.

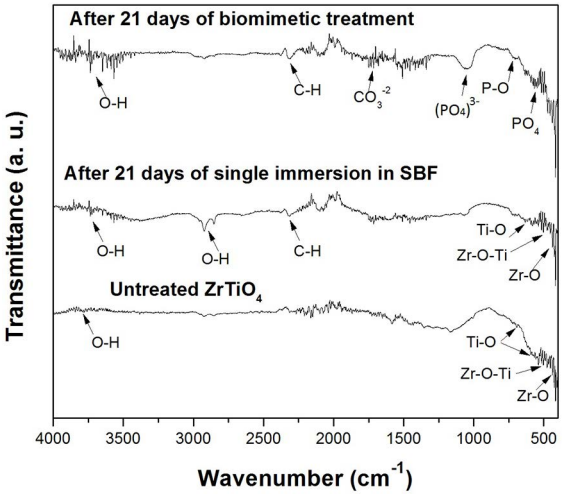

Figure 6. FT-IR spectra of sintered (1500 °C) $ZrTiO_4$: untreated sample, sample after 21 d of immersion in SBF and biomimetically treated sample for 21 d in SBF using a wollastonite powder bed.

In the aim to identify the bioactive compound formed on the surface of biomimetically treated $ZrTiO_4$, TEM and HRTEM analyses were performed (Figure 7). The TEM image (Figure 7) shows the morphology of the material after the biomimetic process. The HRTEM image shows the lattice fringes of (211) and (112) planes of a hydroxyapatite crystal with a lattice spacing of 0.292 and 0.289 nm, respectively. This indicates that the growing layer on $ZrTiO_4$ may correspond to hydroxyapatite, HA [27-30]. In order to verify this information, the chemical composition of the bioactive compound was evaluated by EDS. The resulting analysis revealed a Ca/P ratio = 1.54, which is lower than that of HA (1.67) and very similar to the apatite formed on the existing bioactive systems [27-32]. Thus, the biomimetically treated $ZrTiO_4$ obtained in this work may exhibit a bone-bonding ability through the apatite layer.

4. Conclusions

The viability of using a combination between the mechano-synthesis method and the application of a heat treatment to obtain $ZrTiO_4$ was demonstrated. Results showed that 30 hours of milling followed by heat treatment at 1500 ºC for 6 h are necessary to consider the reactions completed. No bioactive compound was formed on the samples immersed for 21 days in SBF. On the other hand, when a wollastonite powder bed was used during the immersion of samples in SBF, apatite was formed on $ZrTiO_4$ samples. These results indicate that biomimetically treated zirconium titanate may be a potential material for biomedical applications.

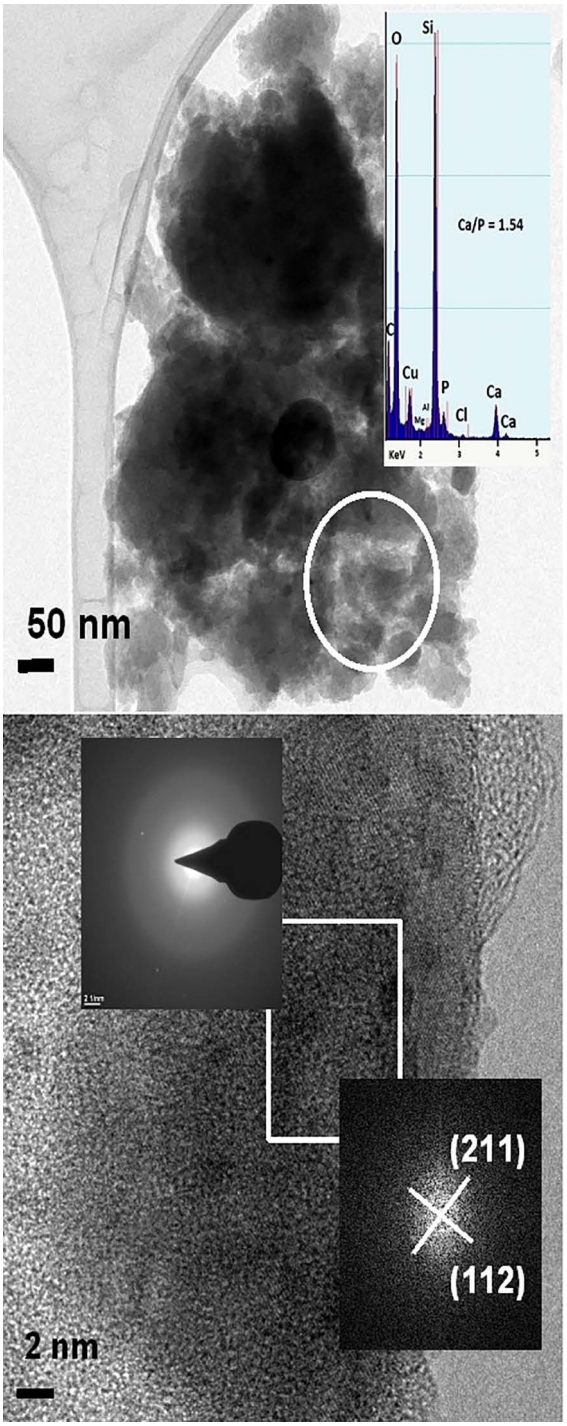

Figure 7. TEM images and EDS spectrum of sintered (1500 ºC) $ZrTiO_4$ after biomimetic treatment for 21 days.

5. Acknowledgements

This work was financially supported by CONACYT (grants CB-2011-01-166 995, PEI 250174 and CB2013-01-221701) and Tecnológico Nacional de México (grant 6798.18-P). D. Rentería -Zamarrón thanks to CONACYT for the posdoctoral scholarship.

6. References

1. Salahinejad E, Hadianfard MJ, Macdonald DD, Sharifi Asl S, Mozafari M, Walker KJ, et al. Surface modification of stainless steel orthopedic implants by Sol-Gel $ZrTiO_4$ and $ZrTiO_4$-PMMA coatings. *Journal of Biomedical Nanotechnology*. 2013;9(8):1327-1335.

2. Akhtar N, Rafique HM, Atiq S, Aslam S, Razaq A, Saleem M. Dielectric based energy storage capacity of sol-gel synthesized Sr-doped $ZrTiO_4$ nanocrystallites. *Ceramics International*. 2018;44(6):6705-6712.

3. Gajović A, Furić M, Musić S, Djerdj I, Tonejc A, Tonejc AM, et al. Mechanism of $ZrTiO_4$ Synthesis by Mechanochemical Processing of TiO_2 and ZrO_2. *Journal of the American Ceramic Society*. 2006;89(7):2196-2205.

4. Fuentes AF, Takacs L. Preparation of multicomponent oxides by mechanochemical methods. *Journal of Materials Science*. 2013;48(2):598-611.

5. George A, Solomon S, Thomas JK, John A. Characterizations and electrical properties of $ZrTiO_4$ ceramic. *Materials Research Bulletin*. 2012;47(11):3141-3147.

6. Park Y, Dim Y. Influence on cooling rate on the physical properties of tin modified zirconium titanate. *Journal of Materials Science Letters*. 1996;15(10):853-855.

7. Kim T, Oh J, Park B, Hong KS. Correlation between strain and dielectric properties in $ZrTiO_4$ thin films. *Applied Physics Letters*. 2000;76(21):3043-3045.

8. Bianco A, Gusmano G, Freer R, Smith P. Zirconium titanate microwave dielectrics prepared via polymeric precursor route. *Journal of the European Ceramic Society*. 1999;19(6-7):959-963.

9. Hirano S, Hayashi T, Hattori A. Chemical Processing and Microwave Characteristics of (Zr,Sn)TiO_4 Microwave Dielectrics. *Journal of the American Ceramic Society*. 1991;74(6):1320-1324.

10. Christoffersen R, Davies PK, Wei X, Negas T. Effect of Sn Substitution on Cation Ordering in $(Zr_{1-x}Sn_x)TiO_4$ Microwave Dielectric Ceramics. *Journal of the American Ceramic Society*. 1994;77(6):1441-1450.

11. Victor P, Bhattacharyya S, Krupanidhi SB. Dielectric relaxation in laser ablated polycrystalline $ZrTiO_4$ thin films. *Journal of Applied Physics*. 2003;94(8):5135-5142.

12. Liu SW, Song CF, Lü MK, Wang SF, Sun DL, Qi YX, et al. A novel $TiO_2/Zr_xTi_{1-x}O_2$ composite photocatalytic films. *Catalysis Communications*. 2003;4(7):343-346.

13. Reddy BM, Khan A. Recent Advances on TiO_2-ZrO_2 Mixed Oxides as Catalysts and Catalyst Supports. *Catalysis Reviews - Science and Engineering*. 2005;47(2):257-296.

14. Mazurkevich YS, Kobasa IM. ZrO_2-TiO_2 Materials. *Inorganic Materials*. 2001;37(12):1285-1288.

15. Sohn JR, Lee SH. Effect of TiO_2-ZrO_2 composition on catalytic activity of supported $NiSO_4$ for ethylene dimerization. *Applied Catalysis A: General*. 2007;321(1):27-34.

16. Costa CEF, Crispim SCL, Lima SJG, Paskocimas CA, Longo E, Fernandes VJ Jr., et al. Synthesis and thermal characterization of zirconium titanate pigments. *Journal of Thermal Analysis and Calorimetry*. 2004;75(2):467-473.

17. Ferrari V, Marioli D, Taroni A, Ranucci E. Multisensor array of mass microbalances for chemical detection based on resonant piezo-layers of screen-printed PZT. *Sensors and Actuators B: Chemical*. 2000;68(1-3):81-87.

18. Gajović A, Šantić A, Djerdj I, Tomašić N, Moguš-Milanković A, Su DS. Structure and electrical conductivity of porous zirconium titanate ceramics produced by mechanochemical treatment and sintering. *Journal of Alloys and Compounds*. 2009;479(1-2):525-531.

19. Williams MC, Strakey JP, Surdoval WA. The U. S. Department of Energy, Office of Fossil Energy Stationary Fuel Cell Program. *Journal of Power Sources*. 2005;143(1-2):191-196.

20. Śmieszek A, Donesz-Sikorska A, Gresiak J, Krzak J, Marycz K. Biological effects of sol-gel derived ZrO_2 and SiO/ZrO_2 coatings on stainless steel surface--In vitro model using mesenchymal stem cells. *Journal of Biomaterials Applications*. 2014;29(5):699-714.

21. Tianinen H, Eder G, Nilsen O, Haugen HJ. Effect of ZrO_2 addition on the mechanical properties of porous TiO_2 bone scaffolds. *Materials Science and Engineering: C*. 2012;32(6):1386-1393.

22. Nogiwa-Valdez AA, Cortés-Hernández DA, Almanza-Robles JM, Chávez-Valdez A. Bioactive Zirconia Composites. *Materials Science Forum*. 2006;509:193-198.

23. Díaz-Guillén JA, Díaz-Guillén MR, Padmasree KP, Fuentes AF, Santamaría J, León C. High ionic conductivity in the pyrochlore-type $Gd_{2-y}La_yZr_2O_7$ solid solution ($0 \leq y \leq 1$). *Solid Ionics*. 2008;179(38):2160-2164.

24. Cortes DA, Nogiwa AA, Almanza JM, Ortega S. Biomimetic apatite coating on Mg-PSZ/Al_2O_3 composites. Effect of the immersion method. *Materials Letters*. 2005;59(11):1352-1355.

25. Ortega-Chavarría S, Cortés-Hernández DA, Nogiwa-Valdez AA. Biomimetic Coating on Zirconia Composites Induced by Chemical Treatment. *Materials Science Forum*. 2007;560:127-132.

26. Liu X, Huang A, Ding C, Chu PK. Bioactivity and cytocompatibility of zirconia (ZrO_2) films fabricated by cathodic arc deposition. *Biomaterials*. 2006;27(21):3904-3911.

27. Dos Santos V, Bergmann CP. Synthesis and Characterization of Crystalline Zirconium Titanate Obtained by Sol-Gel. In Mastai Y, ed. *Advances in Crystallization Processes*. London: IntechOpen; 2012. Available from: http://www.intechopen.com/books/advances-in-crystallizationprocesses/synthesis-and-characterization-of-crystalline-zirconium-titanate-obtained-by-sol-gel

28. Fathi MH, Hanifi A, Mortazavi V. Preparation and bioactivity evaluation of bone-like hydroxyapatite nanopowder. *Journal of Materials Processing Technology*. 2008;202(1-3):536-542.

29. Deng Y, Sun Y, Chen X, Zhu P, Wei S. Biomimetic synthesis and biocompatibility evaluation of carbonated apatites template-mediated by heparin. *Materials Science and Engineering: C*. 2013;33(5):2905-2913.

30. Xiao J, Zhu Y, Ruan Q, Liu Y, Zeng Y, Xu F, et al. Biomacromolecule and Surfactant Complex Matrix for Oriented Stack of 2-Dimensional Carbonated Hydroxyapatite Nanosheets as Alignment in Calcified Tissues. *Crystal Growth and Design*. 2010;10(4):1492-1499.

31. Huang D, Yin M, Lin Q, Qin Y, Wei Y, Hu Y, et al. Aligned hydroxyapatite nano-crystal formation on a polyamide surface. *RSC Advances*. 2017;7(68):43040-43046.

32. Reséndiz-Hernández PJ, Cortés-Hernández DA, Saldívar-Ramírez MMG, Acuña-Gutiérrez IO, Flores-Valdés A, Torres-Rincón S, et al. Novel bioactive materials: silica aerogel and hybrid silica aerogel/pseudo wollastonite. *Boletin de la Sociedad Espanola de Ceramica y Vidrio*. 2014;53(5):235-239.